

A new extended Cardioid model: an application to wind data

Fernanda V. Paula¹, Abraão D. C. Nascimento² and
Getúlio J. A. Amaral²

¹ Colegiado de Matemática, Universidade Federal do Tocantins, Araguaína, TO, Brazil

² Departamento de Estatística, Universidade Federal de Pernambuco, Recife, PE, Brazil

Address for correspondence: Fernanda Vital de Paula, Colegiado de Matemática, Universidade Federal do Tocantins, Araguaína, TO, 77838 – 824, Brazil.

E-mail: fernandavital@uft.edu.br.

Phone: (+55) 63 2112 2227.

Fax: (+55) 63 2112 2349.

Abstract: The Cardioid distribution is a relevant model for circular data. However, this model is not suitable for scenarios where there is asymmetry or multimodality. In order to overcome this gap, an extended Cardioid model is proposed, which is called Exponentiated Cardioid (EC) distribution. Besides, some of its properties are derived, such as trigonometric moments, kurtosis and skewness. A discussion about the modality and expressions for the quantiles through approximations of the

studied model are also presented. To fit the EC model, two estimation methods are presented based on maximum likelihood and quantile least squares procedures. The performance of proposed estimators is evaluated in a Monte Carlo simulation study, adopting both bias and mean square error as comparison criteria. Finally, the proposed model is applied to a dataset in the wind direction context. Results indicate that the EC distribution may outperform Cardioid and the von Mises distributions.

Key words: exponentiated Cardioid; modality; quantiles; trigonometric moments; wind direction

1 Introduction

Circular data have been obtained from various fields, where the measurements are angle and directions, such as in Biology [[Batschelet \(1981\)](#)], Zoology [[Boles and Lohmann \(2003\)](#)], Geology [[Jammalamadaka and Sengupta \(1972\)](#)] and others. Some examples are related to birds navigational, variation in the onset of leukaemia, orientation data in textures and wind directions. The periodic nature of circular data imposes a specific treatment which is appropriate for non-euclidean space. Even though symmetry is assumed by several circular models, there are many practical situations where asymmetric distributions are necessary. Thus, a new tractable flexible circular model will be addressed in this paper.

There are some generators for representing circular and directional data. Among them, the simplest is known as *perturbation procedure* proposed by [Jeffreys \(1961\)](#) and it is based on the product of an existing circular density and a function chosen

such that the resulting expression is also a circular density [Pewsey et. al (2013)]. The cardioid (C) and sine-skewed distributions [Abe and Pewsey (2009)] are particular cases of this method. The C distribution was introduced by Jeffreys (1961) as cosine perturbation of the continuous circular uniform distribution and has probability density function (pdf) given by

$$f_C(\theta) = \frac{1}{2\pi} \{1 + 2\rho \cos(\theta - \mu)\},$$

where $0 \leq \mu < 2\pi$, $|\rho| \leq \frac{1}{2}$ and ρ and μ are concentration and mean direction parameters, respectively. Further, the circular uniform distribution is obtained when $\rho = 0$. Other generator is stemmed from the real line around the circumference, called *wrapping models* [Jammalamadaka and SenGupta (2001)]. The wrapped Cauchy and normal models are examples of this method. Generators defined by transforming the argument of some existing densities, say $g(\theta)$, replacing its argument, θ , by functions of it, can also be mentioned. Some distribution generators in this way are Abe and Pewsey (2013), Jones and Pewsey (2012), Abe et. al (2009) (generated from C) and Batschelet (1981) (from von Mises) families. Moreover, the von Mises distribution is particularly useful in this paper because its wide application to circular data. Its pdf is given by (for $0 \leq \theta < 2\pi$)

$$f_V(\theta) = [2\pi I_0(\rho)]^{-1} \exp[\rho \cos(\theta - \mu)],$$

where $0 \leq \mu < 2\pi$, $\rho \geq 0$ and $I_0(\rho) = \int_0^{2\pi} \exp[\rho \cos(\phi - \mu)] d\phi$ is the modified Bessel function of the first kind and order zero.

A further form to construct a circular model is the called *Möbius transformation*. An example is the proposed family in Kato and Jones (2010), derived from the von Mises distribution. Another method is based on the transformation of a bivariate linear

random variable to its directional component. The obtained models are called *offset* distributions [Mardia (1972)].

The previous generators result generally in symmetrical distributions. However, tractable circular models with asymmetric shape are required in several applications into the circular context. Some asymmetric extensions have been proposed in the literature. Among them, finite mixtures of unimodal models [Mardia (1972)] and the application of multiplicative mixing, as that used by Gatto and Jammalamadaka (2007) to extended the von Mises law. Pewsey et. al (2013) also made reference to the non-negative trigonometric moment distributions [Fernández-Durán (2007)].

In Euclidean space, there are several ways to extend well-defined models. One of them is by exponentiating a cumulative distribution function (cdf), say F , by a positive real number β , $F(\cdot)^\beta$ see; AL-Hussaini and Ahsanullah AL-Hussaini and Ahsanullah (2015). As far as we know, this approach has not been previously used in the circular data context.

In this paper, the methodology described by AL-Hussaini and Ahsanullah AL-Hussaini and Ahsanullah (2015) is used to obtain a new circular distribution, called the *Exponentiated Cardioid* model. The additional parameter may add events of amodality and bimodality to the baseline unimodal C, as will be shown. Expressions for its trigonometric moments are also proposed. Two estimation procedures for the EC parameters are presented: maximum likelihood estimator (MLE) and quantile least squares estimator (QLSE). In order to compare those estimators, a Monte Carlo simulation study is performed, on which we conclude that ML estimates have smaller mean square errors than those of QLS estimates in almost all considered cases. Finally, in order to illustrate the EC distribution potentiality, a comparison of its fit

to those due to C and von Mises distributions is provided. Results of Kuiper and Watson goodness-of-fit statistics present evidence in favor of our proposal.

This paper is organized as follows. In Sections 2 and 3, the EC distribution and some of its mathematical properties are presented. Section 4 deals with estimation procedures. Finally, numerical results obtained from real data studies are presented

2 The Proposed Model

The EC ditribution has cdf given by (for $0 < \theta \leq 2\pi$)

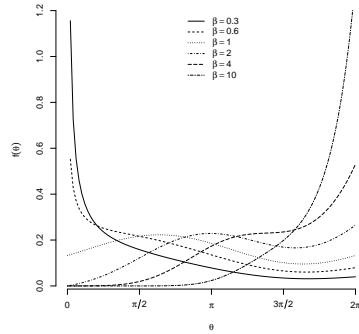
$$F(\theta; \beta, \rho, \mu) = \left\{ \frac{\theta}{2\pi} + \frac{\rho}{\pi} [\sin(\theta - \mu) + \sin(\mu)] \right\}^{\beta}, \quad (2.1)$$

where $0 < \mu \leq 2\pi$, $0 \leq \rho \leq 0.5$ and $\beta > 0$ and, therefore, its pdf is

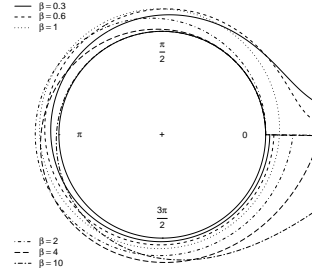
$$f(\theta; \beta, \rho, \mu) = \left\{ \frac{\theta}{2\pi} + \frac{\rho}{\pi} [\sin(\theta - \mu) + \sin(\mu)] \right\}^{\beta-1} \frac{\beta}{2\pi} \{ [1 + 2\rho \cos(\theta - \mu)] \}. \quad (2.2)$$

This situation is denoted as $\Theta \sim EC(\beta, \rho, \mu)$. As special cases, the C distribution follows for $\beta = 1$ and the uniform distribution is obtained when $\beta = 1$ and $\rho = 0$. In this position, it is important to mention that the Cardioid extension by exponentiation requires to the replacement zero by 2π in the EC support comparatively to that of the C model. This change avoids an undefinition at zero.

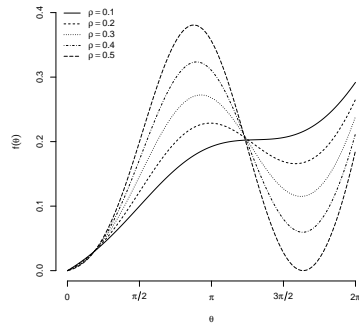
Figure 1 displays EC pdf curves and their associated histograms drawn from generated data for several parametric points. It is noticeable bimodal and asymmetric events in contrast with its baseline at $\beta = 1$. Moreover, higher values of ρ indicate more concentrated scenarios, as illustrated in Figure 1(d).



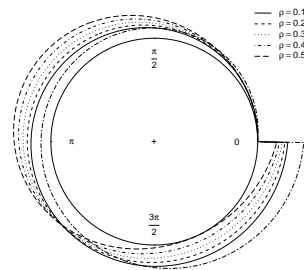
(a) For $\rho = 0.2$ and $\mu = 2$.



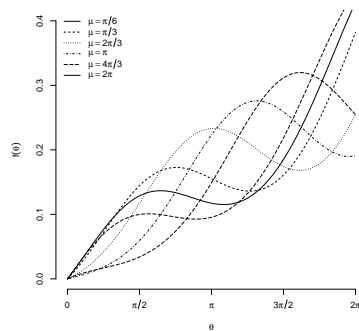
(b) For $\rho = 0.2$ and $\mu = 2$.



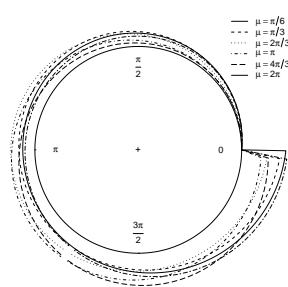
(c) For $\beta = 2$ and $\mu = 2$.



(d) For $\beta = 2$ and $\mu = 2$.



(e) For $\beta = 2$ and $\rho = 0.2$.



(f) For $\beta = 2$ and $\rho = 0.2$.

Figure 1: Theoretical and empirical EC densities for some parametric points.

2.1 Quantiles

Theorem 2.1 *Let $\Theta \sim EC(\beta, \rho, \mu)$. The following expressions are valid for quantiles approximation:*

1. For $Q_\alpha - \mu \in [0, 0.60]$:

$$Q_\alpha \approx \frac{2\pi}{1+2\rho} \left\{ \alpha^{\frac{1}{\beta}} - \frac{\rho}{\pi} [\sin(\mu) - \mu] \right\};$$

2. For $Q_\alpha - \mu \in (0.60, 2.62]$ and $\rho \neq 0$:

$$Q_\alpha \approx \frac{\pi}{\rho} [D - \sqrt{E}];$$

3. For $Q_\alpha - \mu \in (2.62, 3.64]$:

$$Q_\alpha \approx \frac{2\pi}{1-2\rho} \left\{ \alpha^{\frac{1}{\beta}} - \frac{\rho}{\pi} [\sin(\mu) + \mu + \pi] \right\};$$

4. For $Q_\alpha - \mu \in (3.64, 5.76]$ and $\rho \neq 0$:

$$Q_\alpha \approx -\frac{\pi}{\rho} [G - \sqrt{H}];$$

5. For $Q_\alpha - \mu \in (5.76, 6.28]$:

$$Q_\alpha \approx \frac{2\pi}{1+2\rho} \left\{ \alpha^{\frac{1}{\beta}} - \frac{\rho}{\pi} [\sin(\mu) - \mu - 2\pi] \right\};$$

where $C = \alpha^{\frac{1}{\beta}} - \frac{\rho}{\pi} \left\{ \sin(\mu) - \frac{\mu}{2}[\pi + \mu] + \frac{8-\pi^2}{8} \right\}$, $D = \frac{1}{\pi} \left[\frac{1+\pi\rho+2\rho\mu}{2} \right]$, $E = D^2 - \frac{2\rho C}{\pi}$, $G = D - 2\rho \left[1 + \frac{\mu}{\pi} \right]$, $H = G^2 + \frac{2\rho F}{\pi}$ and $F = C - \rho \left[\frac{\mu^2-2}{\pi} + \frac{8\mu+5\pi^2}{4} \right]$.

The EC quantile function (qf) is analytically intractable. However, from trigonometric results and the Taylor serie expansions, approximated expressions for the EC qf may be given, according to Theorem 2.1. The proof is presented in Appendix A.

2.2 Modality Essays

The flexibility of the EC distribution is partially portrayed in Table 1. It knows that the C model ($\beta = 1$) is unimodal. In contrast, the EC distribution can be classified as amodal, unimodal and bimodal for different values of β , ρ and μ . This fact shows our proposal has greater flexibility than its corresponding baseline.

3 Moments

Expressions for the first two trigonometric moments of the EC model are derived in this section. Moreover, standard descriptive measures for the proposed model are obtained from them. In general, EC trigonometric moments do not present closed-form expressions. Thus, they are represented through expansions in terms of a proposed special function as follows.

Theorem 3.1 *Let $\Theta \sim EC(\beta, \rho, \mu)$. Its cdf can be represented as*

$$F(\theta) = \sum_{k=0}^{+\infty} \sum_{s=0}^k T_{k,s} \theta^{\beta-k} [\sin(\theta - \mu)]^s \{ [\sin(\theta - \mu)]^{k-2s} M_0 + [\sin(\mu)]^{k-2s} M_1 \},$$

where $M_0 = I(|\sin(\theta - \mu)| \geq |\sin(\mu)|)$, $M_1 = I(|\sin(\theta - \mu)| < |\sin(\mu)|)$, $I(\cdot)$ refers to the indicator function and $T_{k,s}$ is given by

$$T_{k,s}(\beta, \rho, \mu) = \binom{\beta}{k} \binom{k}{s} \left(\frac{1}{2\pi}\right)^{\beta-k} \left(\frac{\rho}{\pi}\right)^k [\sin(\mu)]^s.$$

It is known, the n th central trigonometric moment of the EC is given by

Table 1: Modality of the EC distribution, for different values of the parameters, where \emptyset =Amodal, \diamond =Unimodal e \blacksquare =Bimodal.

$\beta = 0.3$	ρ				
μ	$\frac{1}{10}$	$\frac{1}{5}$	$\frac{3}{10}$	$\frac{2}{5}$	$\frac{1}{2}$
$\frac{\pi}{6}$	\diamond	\diamond	\diamond	\diamond	\diamond
$\frac{\pi}{3}$	\diamond	\diamond	\diamond	\diamond	\diamond
$\frac{2\pi}{3}$	\diamond	\diamond	\diamond	\diamond	\diamond
π	\emptyset	\emptyset	\emptyset	\emptyset	\emptyset
$\frac{4\pi}{3}$	\emptyset	\diamond	\diamond	\diamond	\diamond
2π	\diamond	\diamond	\diamond	\diamond	\diamond

$\beta = 0.6$	ρ				
μ	$\frac{1}{10}$	$\frac{1}{5}$	$\frac{3}{10}$	$\frac{2}{5}$	$\frac{1}{2}$
$\frac{\pi}{6}$	\diamond	\diamond	\diamond	\diamond	\diamond
$\frac{\pi}{3}$	\diamond	\diamond	\diamond	\diamond	\diamond
$\frac{2\pi}{3}$	\diamond	\diamond	\diamond	\diamond	\blacksquare
π	\emptyset	\diamond	\diamond	\diamond	\diamond
$\frac{4\pi}{3}$	\diamond	\diamond	\diamond	\diamond	\diamond
2π	\diamond	\diamond	\diamond	\diamond	\diamond

$\beta = 1.0$	ρ				
μ	$\frac{1}{10}$	$\frac{1}{5}$	$\frac{3}{10}$	$\frac{2}{5}$	$\frac{1}{2}$
$\frac{\pi}{6}$	\diamond	\diamond	\diamond	\diamond	\diamond
$\frac{\pi}{3}$	\diamond	\diamond	\diamond	\diamond	\diamond
$\frac{2\pi}{3}$	\diamond	\diamond	\diamond	\diamond	\diamond
π	\diamond	\diamond	\diamond	\diamond	\diamond
$\frac{4\pi}{3}$	\diamond	\diamond	\diamond	\diamond	\diamond
2π	\diamond	\diamond	\diamond	\diamond	\diamond

$\beta = 2.0$	ρ				
μ	$\frac{1}{10}$	$\frac{1}{5}$	$\frac{3}{10}$	$\frac{2}{5}$	$\frac{1}{2}$
$\frac{\pi}{6}$	\diamond	\blacksquare	\blacksquare	\blacksquare	\blacksquare
$\frac{\pi}{3}$	\diamond	\blacksquare	\blacksquare	\blacksquare	\blacksquare
$\frac{2\pi}{3}$	\diamond	\blacksquare	\blacksquare	\blacksquare	\blacksquare
π	\blacksquare	\blacksquare	\blacksquare	\blacksquare	\diamond
$\frac{4\pi}{3}$	\diamond	\diamond	\diamond	\blacksquare	\blacksquare
2π	\diamond	\blacksquare	\blacksquare	\blacksquare	\blacksquare

$\beta = 4.0$	ρ				
μ	$\frac{1}{10}$	$\frac{1}{5}$	$\frac{3}{10}$	$\frac{2}{5}$	$\frac{1}{2}$
$\frac{\pi}{6}$	\diamond	\diamond	\blacksquare	\blacksquare	\blacksquare
$\frac{\pi}{3}$	\diamond	\diamond	\blacksquare	\blacksquare	\blacksquare
$\frac{2\pi}{3}$	\diamond	\diamond	\blacksquare	\blacksquare	\blacksquare
π	\diamond	\blacksquare	\blacksquare	\blacksquare	\diamond
$\frac{4\pi}{3}$	\diamond	\diamond	\diamond	\diamond	\diamond
2π	\diamond	\diamond	\blacksquare	\blacksquare	\blacksquare

$\beta = 10.0$	ρ				
μ	$\frac{1}{10}$	$\frac{1}{5}$	$\frac{3}{10}$	$\frac{2}{5}$	$\frac{1}{2}$
$\frac{\pi}{6}$	\diamond	\diamond	\diamond	\blacksquare	\blacksquare
$\frac{\pi}{3}$	\diamond	\diamond	\diamond	\blacksquare	\blacksquare
$\frac{2\pi}{3}$	\diamond	\diamond	\diamond	\blacksquare	\blacksquare
π	\diamond	\diamond	\diamond	\blacksquare	\diamond
$\frac{4\pi}{3}$	\diamond	\diamond	\diamond	\diamond	\diamond
2π	\diamond	\diamond	\diamond	\blacksquare	\blacksquare

$$\mu_p = \mathbb{E}\{\cos[p(\Theta - \mu)]\} + i\mathbb{E}\{\sin[p(\Theta - \mu)]\}.$$

Using integration by parts, it follows that

$$\mathbb{E}\{\cos[p(\Theta - \mu)]\} = \int_0^{2\pi} \cos[p(\theta - \mu)]dF(\theta) = \cos(p\mu) + \int_0^{2\pi} p\{\sin[p(\theta - \mu)]\}F(\theta)d\theta$$

and

$$\mathbb{E}\{\sin[p(\Theta - \mu)]\} = \int_0^{2\pi} \sin[p(\theta - \mu)]dF(\theta) = -\sin(p\mu) - \int_0^{2\pi} p\{\cos[p(\theta - \mu)]\}F(\theta)d\theta$$

When $p = 1$, applying the Theorem 3.1, the EC first moment is given by

$$\mu_1 = \mathbb{E}\{\cos[(\Theta - \mu)]\} + i\mathbb{E}\{\sin[(\Theta - \mu)]\} = \alpha_1 + i\beta_1,$$

where α_1 and β_1 are determined at the following corollary.

Corollary 3.1.1 *Let $\Theta \sim EC(\beta, \rho, \mu)$. The components of the first central trigonometric moment are given by*

$$\alpha_1 = \cos(\mu) + \sum_{k=0}^{+\infty} \sum_{s=0}^k T_{k,s} \{A(\beta - k, 0, k - s + 1)M_0 + [\sin(\mu)]^{k-2s} A(\beta - k, 0, s + 1)M_1\}$$

and

$$\beta_1 = -\sin(\mu) - \sum_{k=0}^{+\infty} \sum_{s=0}^k T_{k,s} \{A(\beta - k, 1, k - s)M_0 + [\sin(\mu)]^{k-2s} A(\beta - k, 1, s)M_1\},$$

where

$$A(a, b, c) = \int_0^{2\pi} \theta^a [\cos(\theta - \mu)]^b [\sin(\theta - \mu)]^c d\theta.$$

Detailed calculations for derivation of the above expressions are presented in Appendix B. To illustrate the use of the Corollary 3.2, for the C distribution ($\beta = 1$, $A(0, 0, 1) = A(0, 1, 1) = A(0, 1, 0) = 0$, $M_0 = 0$ and $M_1 = 1$ or $M_0 = 0$ and $M_1 = 1$), it follows that

$$\begin{aligned} \alpha_1 &= \cos(\mu) + T_{0,0}\{A(1, 0, 1)M_0 + A(1, 0, 1)M_1\} + T_{1,0}\{A(0, 0, 2)M_0 \\ &\quad + \sin(\mu)^{-1}A(0, 0, 1)M_1\} + T_{1,1}\{A(0, 0, 1)M_0 + \sin(\mu)^{-1}A(0, 0, 2)M_1\} \\ &= \cos(\mu) + (2\pi)^{-1}\{-2\pi \cos(\mu)(M_0 + M_1)\} + \frac{\rho}{\pi}\pi M_0 + \frac{\rho \sin(\mu)}{\pi}[\pi \sin(\mu)^{-1}]M_1 \\ &= \rho \end{aligned}$$

and

$$\begin{aligned} \beta_1 &= -\sin(\mu) - T_{0,0}\{A(1, 1, 0)M_0 + A(1, 1, 0)M_1\} - T_{1,0}\{A(0, 1, 1)M_0 \\ &\quad + \sin(\mu)A(0, 1, 0)M_1\} - T_{1,1}\{A(0, 1, 0)M_0 + \sin(\mu)^{-1}A(0, 1, 1)M_1\} \\ &= -\sin(\mu) + (2\pi)^{-1}\{2\pi \sin(\mu)(M_0 + M_1)\} \\ &= 0, \end{aligned}$$

which corresponds to the components of the first central trigonometric moment of the C distribution [Fisher (1993)]. In a similar manner, the second moment is

$$\mu_2 = \mathbb{E}\{\{\cos[2(\Theta - \mu)]\}\} + i\mathbb{E}\{\{\sin[2(\Theta - \mu)]\}\} = \alpha_2 + i\beta_2,$$

where α_2 and β_2 are determined as follows.

Corollary 3.1.2 *Let $\Theta \sim EC(\beta, \rho, \mu)$. The components of the second central trigonometric moment are given by*

$$\begin{aligned} \alpha_2 &= \cos(2\mu) + 4 \sum_{k=0}^{\infty} \sum_{s=0}^k T_{k,s}\{A(\beta - k, 1, k - s + 1)M_0 \\ &\quad + [\sin(\mu)]^{k-2s}A(\beta - k, 1, s + 1)M_1\} \end{aligned}$$

and

$$\beta_2 = -\sin(2\mu) - 2 \sum_{k=0}^{\infty} \sum_{s=0}^k T_{k,s} \{ [2A(\beta - k, 2, k - s) - A(\beta - k, 0, k - s)] M_0 + [\sin(\mu)]^{k-2s} [2A(\beta - k, 2, s) - A(\beta - k, 0, s)] M_1 \}.$$

Table 2: Ranges of some standard circular measures of the EC distribution.

Measure	Expression	Range
Mean Resultant Length	ρ_1	$[0, 1]$
Circular Variance	$1 - \rho_1$	$[0, 1]$
Circular Standard Deviation	$\sqrt{-2 \log \rho_1}$	$[0, \infty)$
Circular Dispersion	$(1 - \alpha_2)/(2\rho_1^2)$	$[0, \infty)$
Circular Skewness	$\beta_2/(1 - \rho_1)^{\frac{3}{2}}$	$(-\infty, \infty)$
Circular Kurtosis	$(\alpha_2 - \rho_1^4)/(1 - \rho_1)^2$	$(-\infty, \infty)$

Some standard circular measures are functions of the first and second trigonometric moments. The second column of Table 2 presents expressions (in terms of ρ_1 , α_2 and β_2) for mean resultant length, circular variance, standard deviation, dispersion, skewness and kurtosis of any circular model. Using results of Corollaries 3.1.1 and 3.1.2, these quantities can be obtained to the EC model. The ranges to each resulting EC quantities are given in the third column of Table 2. The used notation is the same as in Fisher (1993), where $\rho_i = \sqrt{\alpha_i^2 + \beta_i^2}$ for $i = 1, 2$.

In order to illustrate the presented measures, Figure 2 displays the plots of skewness and kurtosis of C, EC and von Mises distributions, which characterize the distribution

shape. It may be observed the C (skewness, kurtosis) pair is overlapped to that of the von Mises law and the EC pair region covers the two first. From perspective of this diagram, our model seems to extend the former models. Additionally, C and von Mises skewnesses assume null values, as expected.

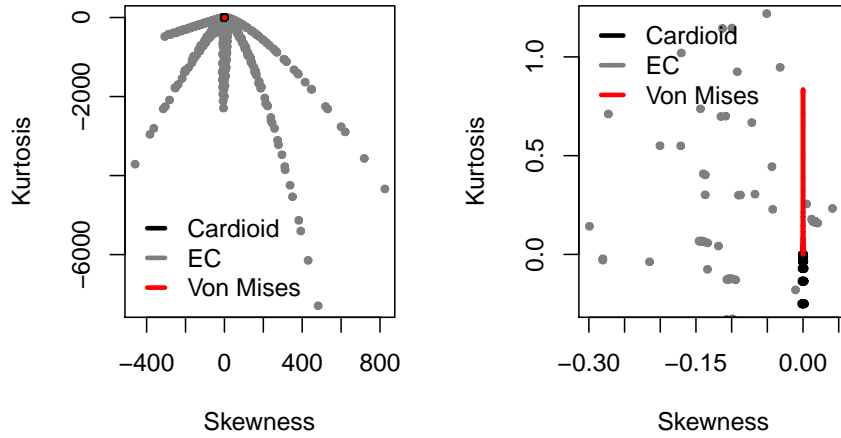


Figure 2: Skewness and kurtosis maps for EC, C and von Mises distributions.

4 Estimation Procedures

4.1 Maximum Likelihood Estimation

Let $\theta_1, \theta_2, \dots, \theta_n$ be a n -points observed sample from $\Theta \sim \text{EC}(\beta, \rho, \mu)$. Then the log-likelihood function at $\boldsymbol{\delta} = (\beta, \rho, \mu)^\top$ is given by

$$\begin{aligned}
 l(\boldsymbol{\delta}) = & n \log \beta + (\beta - 1) \sum_{i=1}^n \log \left\{ \frac{\theta_i}{2\pi} + \frac{\rho}{\pi} [\sin(\theta_i - \mu) + \sin \mu] \right\} \\
 & - n \log(2\pi) + \sum_{i=1}^n \log \{1 + 2\rho \cos(\theta_i - \mu)\}.
 \end{aligned}$$

Therefore, the ML estimates for β , ρ and μ , say $\hat{\beta}$, $\hat{\rho}$ and $\hat{\mu}$, can be defined as solutions of the following non-linear system:

$$\left. \frac{\partial l(\boldsymbol{\delta})}{\partial \beta} \right|_{\boldsymbol{\delta}=\hat{\boldsymbol{\delta}}} = \frac{n}{\beta} + \sum_{i=1}^n \log \left\{ \frac{\theta_i}{2\pi} + \frac{\rho}{\pi} [\sin(\theta_i - \mu) + \sin \mu] \right\} = 0, \quad (4.1)$$

$$\left. \frac{\partial l(\boldsymbol{\delta})}{\partial \rho} \right|_{\boldsymbol{\delta}=\hat{\boldsymbol{\delta}}} = \sum_{i=1}^n \left\{ (\beta - 1) \frac{\sin(\theta_i - \mu) + \sin \mu}{\theta_i + 2\rho[\sin(\theta_i - \mu) + \sin \mu]} + \frac{\cos(\theta_i - \mu)}{1 + 2\rho \cos(\theta_i - \mu)} \right\} = 0 \quad (4.2)$$

and

$$\left. \frac{\partial l(\boldsymbol{\delta})}{\partial \mu} \right|_{\boldsymbol{\delta}=\hat{\boldsymbol{\delta}}} = \sum_{i=1}^n \left\{ (\beta - 1) \frac{-\cos(\theta_i - \mu) + \cos \mu}{\theta_i + 2\rho[\sin(\theta_i - \mu) + \sin \mu]} + \frac{\sin(\theta_i - \mu)}{1 + 2\rho \cos(\theta_i - \mu)} \right\} = 0. \quad (4.3)$$

This system can be reduced to others under equations (4.2) and (4.3), replacing the ML estimate $\hat{\beta}$ by

$$\hat{\beta}(\rho, \mu) = -\frac{n}{\sum_{i=1}^n \log \left\{ \frac{\theta_i}{2\pi} + \frac{\rho}{\pi} [\sin(\theta_i - \mu) + \sin \mu] \right\}}, \quad (4.4)$$

which is obtained from (4.1). Thus, the ML estimates for ρ and μ are obtained numerically from $\left. \frac{\partial l(\boldsymbol{\delta})}{\partial \rho} \right|_{\boldsymbol{\delta}=\hat{\boldsymbol{\delta}}} = 0$ and $\left. \frac{\partial l(\boldsymbol{\delta})}{\partial \mu} \right|_{\boldsymbol{\delta}=\hat{\boldsymbol{\delta}}} = 0$.

4.2 Quantile Least Squares Method

The QLSE for $\boldsymbol{\delta}$ can be defined as solutions from minimization of the sum of squares of the differences between theoretical and empirical quantiles. Consider $\theta_{1:n}, \dots, \theta_{n:n}$ as observed order statistics drawn from n -points random sample of $\Theta \sim EC(\beta, \rho, \mu)$, where $\theta_{k:n}$ is the k th order statistics. Thus, the QLS estimates for EC parameters consist in argument that minimizes the following goal function:

$$q(\boldsymbol{\delta}) = \sum_{i=1}^n \left[\frac{i}{n} - \left\{ \frac{\theta_{i:n}}{2\pi} + \frac{\rho}{\pi} [\sin(\theta_{i:n} - \mu) + \sin(\mu)] \right\}^\beta \right]^2. \quad (4.5)$$

Equivalently to discussed in previous section, the QLS estimates for β , ρ and μ can be defined as solutions of the following non-linear equations system:

$$\frac{\partial q(\boldsymbol{\delta})}{\partial \beta} = \sum_{i=1}^n \left[\frac{i}{n} - F(\theta_{i:n}) \right] F_C(\theta_{i:n})^{2\beta-1} \log[F_C(\theta_{i:n})] = 0, \quad (4.6)$$

$$\frac{\partial q(\boldsymbol{\delta})}{\partial \rho} = \sum_{i=1}^n \left[\frac{i}{n} - F(\theta_{i:n}) \right] F_C(\theta_{i:n})^{\beta-1} \frac{1}{\pi} [\sin(\theta_{i:n} - \mu) + \sin \mu] = 0 \quad (4.7)$$

and

$$\frac{\partial q(\boldsymbol{\delta})}{\partial \mu} = \sum_{i=1}^n \left[\frac{i}{n} - F(\theta_{i:n}) \right] F_C(\theta_{i:n})^{\beta-1} \frac{\rho}{\pi} [\cos(\theta_{i:n} - \mu) - \cos \mu] = 0, \quad (4.8)$$

where F_C represents the C cdf and F is given in (2.1).

5 Numerical Results

5.1 Simulation Study

First, a Monte Carlo simulation study was performed to assess and compare the two proposed estimators. To that end, five thousand replications were considered and, on each one of them, bias and mean square error for both procedures were quantified, like comparison criteria.

Initially, a discussion about the effect of using (6) is presented in estimation process by maximum likelihood. Here, a sample size $n = 100$ and four parametric points are considered. Results are displayed in Table 3 and indicate that the use of (6) may imply in more accurate estimates. The most pronounced improvement can be observed to estimate ρ . Moreover, the estimation considering (6) takes a mean execution of 83 seconds, while the other is slower, taking 116 seconds. From now on, the best ML estimates for β , ρ and μ will be used.

Table 3: MSEs for the ML estimates using as estimation system (4.1)-(4.3) labelled as “MSEa” and (4.4) in (4.2)-(4.3) denoted as “MSEb” are considered. The size of the sample and Monte Carlo replications were set to 100 and 5.000, respectively.

(β, ρ, μ)	MSEa	MSEb
$(1, \frac{1}{2}, 2\pi)$	(0.0071, 0.2991, 0.0000)	(0.0000, 0.0000, 0.0000)
$(4, \frac{3}{10}, \frac{2\pi}{3})$	(0.6449, 13.7865, 0.0764)	(0.5101, 0.0030, 0.0516)
$(1, \frac{3}{10}, \frac{4\pi}{3})$	(0.0658, 0.5818, 0.1883)	(0.0293, 0.0073, 0.0936)
$(4, \frac{1}{2}, \frac{\pi}{3})$	(0.2384, 11.4078, 0.0119)	(0.1761, 0.0001, 0.0056)

Now, methods discussed in previous sections are compared. Results are presented in Tables 4 and 5. They are indexed in terms of mean direction and resultant length under ascending order for $n = 30, 50$ and 100 . In regard to choose parametric scenarios, vectors (β, ρ, μ) are selected such that they have different mean directions and resultant lengths.

Figures 3 and 5 show the MSEs for the ML and QLS estimates at parameter vectors of Table 4 added to other four, respectively. Figures 4 and 6 also address MSEs for points in Table 5 along with ones. To illustrate the abscissas of graphs, Figure 3 begins with $(0.6, 0.2, \frac{\pi}{6})$ with mean direction 0.0279 and, after, by $(2, 0.3, \frac{2\pi}{3})$ with mean direction 1.1777.

Table 4: Average bias e average MSE for the ML and QLS estimates for different values of β , ρ and μ , by the Monte Carlo method, over 5.000 replications. The size of the sample was set to 30, 50 and 100. The parametric vectors of the first column are sorted by mean direction.

(β, ρ, μ)	Method	n	Bias	MSE
$(1, \frac{1}{2}, 2\pi)$	MLE	30	(0.0315, 0.0000, 0.0000)	(0.0272, 0.3683, 0.0000)
		50	(0.0170, 0.0000, 0.0000)	(0.0000, 0.0000, 0.0000)
		100	(0.0094, 0.0000, 0.0000)	(0.0000, 0.0000, 0.0000)
	QLSE	30	(0.0685, 0.0000, 0.0000)	(0.0213, 0.3398, 0.0000)
		50	(0.0546, 0.0000, 0.0000)	(0.0129, 0.3176, 0.0000)
		100	(0.0421, 0.0000, 0.0000)	(0.0071, 0.2991, 0.0000)
$(1, \frac{3}{10}, \frac{4\pi}{3})$	MLE	30	(0.1343, 0.0128, -0.1473)	(0.2093, 0.0173, 0.5766)
		50	(0.0703, 0.0011, -0.0873)	(0.0842, 0.0126, 0.2838)
		100	(0.0330, -0.0030, -0.0361)	(0.0293, 0.0073, 0.0936)
	QLSE	30	(0.0823, 0.0419, -0.1351)	(0.3230, 0.9282, 0.5750)
		50	(0.0337, 0.0254, -0.1035)	(0.1420, 0.6792, 0.3726)
		100	(0.0185, 0.0104, -0.0679)	(0.0658, 0.5818, 0.1883)
$(4, \frac{1}{2}, \frac{\pi}{3})$	MLE	30	(0.0683, -0.0089, -0.0067)	(0.6570, 0.0006, 0.0215)
		50	(0.0249, -0.0068, -0.0045)	(0.3651, 0.0003, 0.0123)
		100	(0.0112, -0.0041, -0.0025)	(0.1761, 0.0001, 0.0056)
	QLSE	30	(-0.3654, -0.0311, -0.0570)	(1.0033, 10.6952, 0.0581)
		50	(-0.2616, -0.0236, -0.0362)	(0.4815, 10.9000, 0.0293)
		100	(-0.1544, -0.0165, -0.0191)	(0.2384, 11.4078, 0.0119)

Table 5: Average bias e MSE for the ML and QLS estimates for different values of β , ρ and μ , by the Monte Carlo method, over 5.000 replications. The size of the sample was set to 30, 50 and 100. The parametric vectors of the first column are sorted by mean resultant length.

(β, ρ, μ)	Method	n	Bias	MSE
$(0.3, \frac{1}{2}, \frac{4\pi}{3})$	MLE	30	(0.0131, -0.0076, 0.0135)	(0.0041, 0.0007, 0.0242)
		50	(0.0069, -0.0049, 0.0017)	(0.0021, 0.0002, 0.0113)
		100	(0.0036, -0.0029, -0.0035)	(0.0010, 0.0001, 0.0048)
	QLSE	30	(0.0064, -0.0219, -0.0045)	(0.0098, 0.0185, 0.0739)
		50	(0.0038, -0.0156, 0.0017)	(0.0035, 0.0128, 0.0378)
		100	(0.0036, -0.0111, 0.0043)	(0.0012, 0.0105, 0.0191)
$(4, \frac{3}{10}, \frac{\pi}{3})$	MLE	30	(0.3223, 0.0178, 0.0031)	(1.5698, 0.0096, 0.1673)
		50	(0.1696, 0.0106, -0.0062)	(0.7629, 0.0060, 0.0969)
		100	(0.0852, 0.0050, -0.0052)	(0.3411, 0.0032, 0.0440)
	QLSE	30	(-0.0977, 0.0034, -0.1103)	(3.2670, 15.5235, 0.3313)
		50	(-0.1147, 0.0027, -0.1092)	(1.1496, 13.9908, 0.1954)
		100	(-0.0603, 0.0006, -0.0639)	(0.5405, 13.7842, 0.0832)
$(10, \frac{1}{2}, 2\pi)$	MLE	30	(0.3154, 0.0000, 0.0000)	(3.9682, 0.0000, 0.0000)
		50	(0.1698, 0.0000, 0.0000)	(2.1771, 0.0000, 0.0000)
		100	(0.0935, 0.0000, 0.0000)	(1.0645, 0.0000, 0.0000)
	QLSE	30	(0.3048, 0.0000, 0.0000)	(0.2787, 96.3191, 0.0000)
		50	(0.3012, 0.0000, 0.0000)	(0.2685, 96.2410, 0.0000)
		100	(0.2861, 0.0000, 0.0000)	(0.2405, 95.9267, 0.0000)

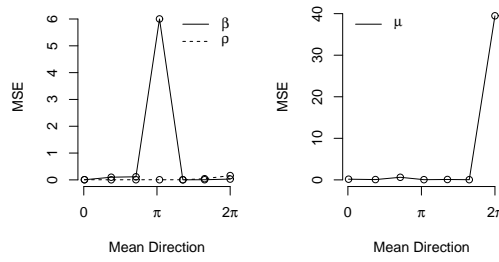


Figure 3: MSE for the ML estimates of the seven parametric vectors chosen according to the mean direction.

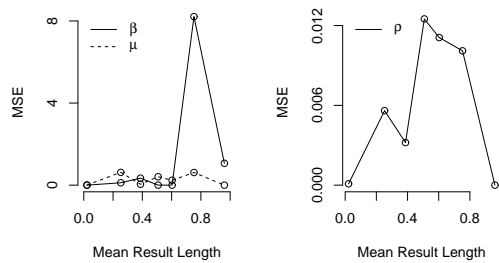


Figure 4: MSE for the ML estimates of the seven parametric vectors chosen according to the mean resultant length.

In regard to variation of mean direction, fourth and seventh points impose difficulties to both methods for estimating the parameters. However, the impact over ML estimates are smaller than that on the QLS estimates. For the variation of mean resultant length, the hardest scenario is the sixth point and the same conclusion is obtained. In particular, poor QLS estimates for ρ at third, sixth and seventh points are found, according to Figure 6, in contrast with respective ML estimates. Additionally, such points refer to $\beta = 4$, $\beta = 4$ and $\beta = 10$, respectively, which indicates that high values to β difficult the estimation of ρ .

Interesting evidence can be found in Figure 6, where the behavior of MSEs for esti-

mates of ρ is approximately monotone.

In general, the MLE performed better than the QLSE in most considered cases, comparing the MSEs of the estimates. The QLSE seems to be more indicated for large β ($\beta = 10$) and small ρ ($\rho = \frac{1}{5}$) (see Table 6).

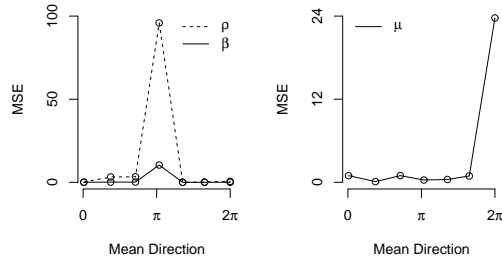


Figure 5: MSE for the QLS estimates of the seven parametric vectors chosen according to the mean direction.

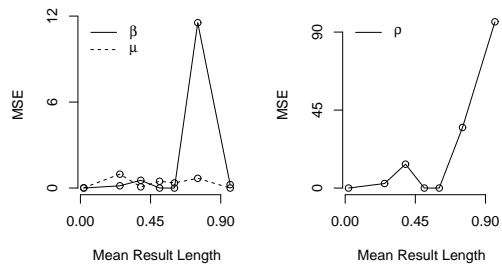


Figure 6: MSE for the QLS estimates of the seven parametric vectors chosen according to the mean resultant length.

Table 6: Average EQM for the ML and QLS estimates for different values of β , ρ and μ , by the Monte Carlo method, over 5.000 replications and sample size $n = 100$.

(β, ρ, μ)	ML	QLS
$(0.3, \frac{1}{5}, \frac{2\pi}{3})$	(0.0014, 0.0125, 0.4106)	(0.0019, 0.0104, 0.4729)
$(0.3, \frac{1}{5}, \frac{\pi}{6})$	(0.0011, 0.0111, 0.2384)	(0.0013, 0.0106, 0.3574)
$(10, \frac{1}{2}, 2\pi)$	(1.0645, 0.0000, 0.0000)	(0.2405, 95.9267, 0.0000)

5.2 Application

In order to illustrate the potentiality of the EC distribution, an application to real data was made. Further, its performance was compared with other due to the Cardioid and von Mises models. ML estimates were used to fit considered models to data. All the computations were done using function `maxLik` at the R statistical software [R Core Team (2015)].

The dataset consists of 21 wind directions obtained by a Milwaukee weather station, at 6.00 am on consecutive days [Johnson and Wehrly (1977)] (see Appendix C). The independence of the data can be verified by the Box-Pierce (Ljung-Box) test [Box and Pierce (1970)] in Figure 7.

The Figure 8 shows the sample skewness and kurtosis of data, by the blue point given by 0.4313 and 0.2480, respectively. It noticeable that the EC model may provide better fit than those due to C and von Mises distributions. The likelihood ratio test was also applied to compare the C ($H_0 : \beta = 1$) and EC ($H_0 : \beta \neq 1$) distributions. The p-value is 0.0027, indicating the EC model as the best descriptor for these wind directions. In what follows, other quantitative discussions are done.

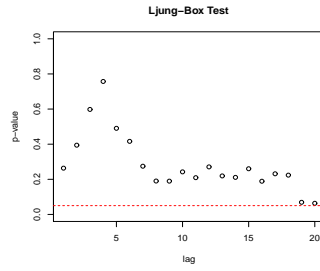


Figure 7: Ljung-Box test statistic.

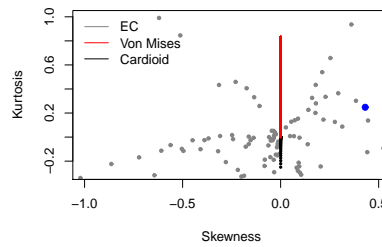


Figure 8: Data skewness and kurtosis.

First, the ML estimates and their SEs (given in parentheses) are evaluated and, subsequently, the values of the Kuiper (K) and Watson (W) statistics are obtained. These adherence measures may be found in [Jammalamadaka and SenGupta \(2001\)](#) and they are given by

$$K = \sqrt{n} \left\{ \max_{1 \leq i \leq n} \left(U_{(i)} - \frac{i-1}{n} \right) + \max_{1 \leq i \leq n} \left(\frac{i}{n} - U_{(i)} \right) \right\}$$

and

$$W = \sum_{i=1}^n \left[\left(U_{(i)} - \frac{i-0.5}{n} \right) - (\bar{U} - 0.5) \right]^2 + \frac{1}{12n},$$

where $U_{(i)} = F(\alpha_{(i)})$ in terms of the ordered observations $\alpha_{(1)} \leq \alpha_{(2)} \leq \dots \leq \alpha_{(n)}$. In general, smaller values of them are associated to better fits. Table 7 displays results from where we concluded that the EC distribution could be chosen as the best model for the data set.

In order to do a qualitative comparison, Figure 9 presents empirical and fitted densities. Results confirm what is concluded from Table 7.

Table 7: ML estimates of the model parameters for the data, the corresponding standard errors (given in parentheses) and the Kuiper and Watson statistics.

Model	β	ρ	μ	Kuiper	Watson
Cardioid	—	0.2436 (0.1463)	4.6708 (0.6835)	1.0388	0.0592
Exponentiated Cardioid	2.8757 (0.8929)	0.2164 (0.1465)	1.1782 (0.6168)	0.7369	0.0257
Von Mises	—	0.5322 (0.3250)	5.0092 (0.5899)	1.1590	0.0711

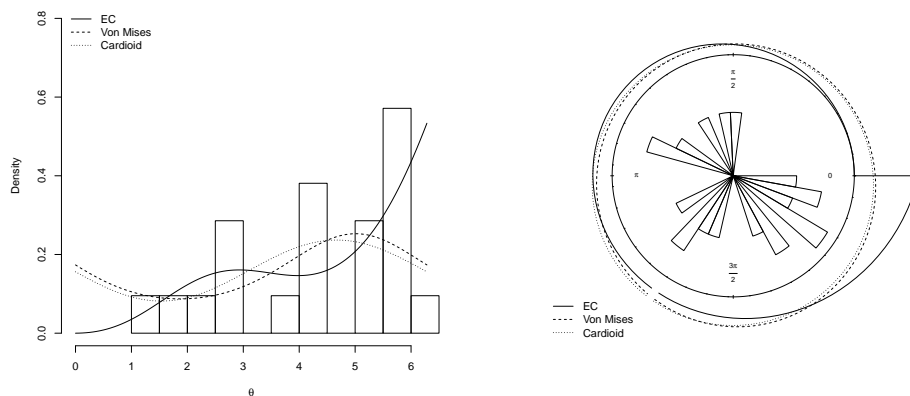


Figure 9: Fitted densities of the EC, C and von Mises models for the real data.

6 Concluding remarks

An extended cardioid model has been proposed, called the *Exponentiated Cardioid* distribution. Our proposal has shown to be able to describe circular asymmetric data, as well as amodality, unimodality and bimodality scenarios. Expressions for the EC trigonometric moments by means of expansions were derived and a discussion about its quantile function and mode was presented. Two estimation procedures for the EC parameters were proposed in regard to maximum likelihood and quantile least square frameworks. The performance of these estimates was quantified through a Monte Carlo simulation study. Finally, an application to real wind data was made and results have indicated that the EC model may outperform the classic C and von Mises distributions.

Appendix

A The proof of Theorem 2.1.

Let $\Theta \sim EC(\beta, \rho, \mu)$. For $\theta \in [0, 0.6]$, $\theta \approx \sin(\theta)$. Thus, $\theta - \mu \approx \sin(\theta - \mu)$, for $\theta - \mu \in [0, 0.6]$. In this case, being $\theta = Q_\alpha$, where Q_α is the EC quantil at α , it follows from (1):

$$\begin{aligned}
 \alpha &= \left\{ \frac{Q_\alpha}{2\pi} + \frac{\rho}{\pi} [\sin(Q_\alpha - \mu) + \sin(\mu)] \right\}^\beta \Rightarrow \alpha^{\frac{1}{\beta}} = \frac{Q_\alpha}{2\pi} + \frac{\rho}{\pi} [\sin(Q_\alpha - \mu) + \sin(\mu)] \\
 &\Rightarrow \alpha^{\frac{1}{\beta}} \approx \frac{Q_\alpha}{2\pi} + \frac{\rho}{\pi} [Q_\alpha - \mu + \sin(\mu)] \Rightarrow \alpha^{\frac{1}{\beta}} + \frac{\rho}{\pi} [\mu - \sin(\mu)] \approx \frac{Q_\alpha}{2\pi} (1 + 2\rho) \\
 &\Rightarrow Q_\alpha \approx \frac{2\pi}{1 + 2\rho} \left\{ \alpha^{\frac{1}{\beta}} + \frac{\rho}{\pi} [\mu - \sin(\mu)] \right\}.
 \end{aligned}$$

The items (3) and (5) of this Theorem are demonstrated in a similar way.

Now, let $\Theta \sim EC(\beta, \rho, \mu)$. For $\theta \in [0.6, 2.62]$, the quadratic function $-\frac{1}{2}\theta^2 + \frac{\pi}{2}\theta + \frac{8-\pi^2}{8} \approx \sin(\theta)$ obtained from the second degree Taylor polynomial for $\sin(\theta)$ around the value $\frac{\pi}{2}$ is used. Thus, $-\frac{1}{2}(\theta - \mu)^2 + \frac{\pi}{2}(\theta - \mu) + \frac{8-\pi^2}{8} \approx \sin(\theta - \mu)$, for $\theta - \mu \in [0.6, 2.62]$.

In this case,

$$\begin{aligned}
 \alpha &= \left\{ \frac{Q_\alpha}{2\pi} + \frac{\rho}{\pi} [\sin(Q_\alpha - \mu) + \sin(\mu)] \right\}^\beta \Rightarrow \alpha^{\frac{1}{\beta}} = \frac{Q_\alpha}{2\pi} + \frac{\rho}{\pi} [\sin(Q_\alpha - \mu) + \sin(\mu)] \\
 &\Rightarrow \alpha^{\frac{1}{\beta}} \approx \frac{Q_\alpha}{2\pi} + \frac{\rho}{\pi} \left[-\frac{1}{2}(Q_\alpha - \mu)^2 + \frac{\pi}{2}(Q_\alpha - \mu) + \frac{8 - \pi^2}{8} + \sin(\mu) \right] \\
 &\Rightarrow \alpha^{\frac{1}{\beta}} - \frac{\rho}{\pi} \sin(\mu) - \frac{\pi}{\rho} \left\{ \frac{\mu}{2} [-\mu - \pi] + \frac{8 - \pi^2}{8} \right\} \approx -\frac{\rho}{2\pi} Q_\alpha^2 + \left\{ \frac{1}{\pi} \left[\frac{1}{2} + \rho\mu + \frac{\pi\rho}{2} \right] \right\} Q_\alpha.
 \end{aligned}$$

Let $C = \alpha^{\frac{1}{\beta}} - \frac{\rho}{\pi} \sin(\mu) - \frac{\pi}{\rho} \left\{ \frac{\mu}{2} [-\mu - \pi] + \frac{8-\pi^2}{8} \right\}$ and $D = \frac{1}{\pi} \left[\frac{1}{2} + \rho\mu + \frac{\pi\rho}{2} \right]$, then

$$-\frac{\rho}{2\pi} Q_\alpha^2 + DQ_\alpha - C \approx 0 \Rightarrow Q_\alpha \approx \frac{\pi}{\rho} [D - \sqrt{E}],$$

where $E = D^2 - \frac{2\rho C}{\pi}$.

The item 4 of the theorem is demonstrated in a similar manner. In this case, $\frac{1}{2}\theta^2 - \frac{3\pi}{2}\theta + \frac{9\pi^2-8}{8}$ is the second degree Taylor polynomial for $\sin(\theta)$ around the value $\frac{3\pi}{2}$.

As an illustration, the Figure 10 shows the plot of $\sin(\theta)$ and the functions used for the approximations.

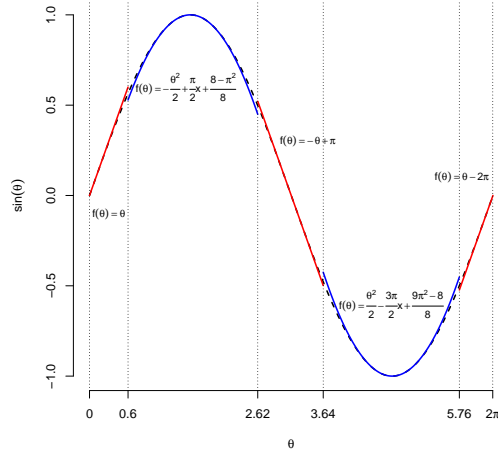


Figure 10: Functions that approximate $\sin(\theta)$ and respective intervals of variation.

B First central trigonometric moment

In this appendix, the expression for the first central trigonometric moment of the EC distribution is derived in detail.

Theorem B.1 (Binomial Theorem) *It is known, for $r \in \mathbb{R}$ ou $|\frac{x}{y}| < 1$,*

$$(x + y)^r = \sum_{k=0}^{\infty} \binom{r}{k} x^k y^{r-k}.$$

Consider also the following trigonometric inequalities and relation: For $x \in \mathbb{R}$, i) $|\sin(x)| < x$ and $|\cos(x)| < 1$ and ii) $\sin(x) + \cos(y) = 2 \sin\left(\frac{x+y}{2}\right) \cos\left(\frac{x-y}{2}\right)$ hold and, consequently, one has that

$$\begin{aligned} \left| \frac{\frac{\rho}{\pi} [\sin(\theta - \mu) + \sin(\mu)]}{\frac{\theta}{2\pi}} \right| &= \left| \frac{2\rho [\sin(\theta - \mu) + \sin(\mu)]}{\theta} \right| = \left| \frac{4\rho}{\theta} \sin\left(\frac{\theta}{2}\right) \cos\left(\frac{\theta - 2\mu}{2}\right) \right| \\ &< \left| \frac{4\rho}{\theta} \frac{\theta}{2} \cos\left(\frac{\theta - 2\mu}{2}\right) \right| \leq 2\rho \leq 1. \end{aligned}$$

Thus, from the binomial theorem, the EC cdf can be written as

$$\left\{ \frac{\theta}{2\pi} + \frac{\rho}{\pi} [\sin(\theta - \mu) + \sin(\mu)] \right\}^\beta = \sum_{k=0}^{\infty} \binom{\beta}{k} \left(\frac{\theta}{2\pi} \right)^{\beta-k} \left(\frac{\rho}{\pi} \right)^k [\sin(\theta - \mu) + \sin(\mu)]^k.$$

Further, the term $[\sin(\theta - \mu) + \sin(\mu)]^k$ may be rewritten as

$$\begin{aligned} & [\sin(\theta - \mu)]^k \left[1 + \frac{\sin(\mu)}{\sin(\theta - \mu)} \right]^k M_0 + [\sin(\mu)]^k \left[1 + \frac{\sin(\theta - \mu)}{\sin(\mu)} \right]^k M_1 \\ &= [\sin(\theta - \mu)]^k \sum_{s=0}^{+\infty} \binom{k}{s} \left[\frac{\sin(\mu)}{\sin(\theta - \mu)} \right]^s M_0 + [\sin(\mu)]^k \sum_{s=0}^{+\infty} \binom{k}{s} \left[\frac{\sin(\theta - \mu)}{\sin(\mu)} \right]^s M_1, \end{aligned}$$

where, $M_0 = I(|\sin(\theta - \mu)| \geq |\sin(\mu)|)$, $M_1 = I(|\sin(\theta - \mu)| < |\sin(\mu)|)$, $I(\cdot)$ refers to the indicator function and the portion composed by the quotients are, in module, less than 1. Thus, from the Binomial theorem, it follows that

$$F(\theta) = \sum_{k=0}^{+\infty} \sum_{s=0}^k \binom{\beta}{k} \binom{k}{s} \left(\frac{\theta}{2\pi} \right)^{\beta-k} \left(\frac{\rho}{\pi} \right)^k \left\{ \frac{\sin(\mu)^s}{\sin(\theta - \mu)^{s-k}} M_0 + \frac{\sin(\theta - \mu)^s}{\sin(\mu)^{s-k}} M_1 \right\}.$$

To simplify this expression, we adopt the notation

$$T_{k,s}(\beta, \rho, \mu) = \binom{\beta}{k} \binom{k}{s} \left(\frac{1}{2\pi} \right)^{\beta-k} \left(\frac{\rho}{\pi} \right)^k [\sin(\mu)]^s.$$

Thus,

$$F(\theta) = \sum_{k=0}^{\infty} \sum_{s=0}^k T_{k,s} \theta^{\beta-k} [\sin(\theta - \mu)]^s \{ [\sin(\theta - \mu)]^{k-2s} M_0 + [\sin(\mu)]^{k-2s} M_1 \}.$$

Now, using integration by parts, the EC p th central trigonometric moment is given

by

$$\begin{aligned}\mu_p &= \mathbb{E}\{\cos[p(\Theta - \mu)]\} + i\mathbb{E}\{\sin[p(\Theta - \mu)]\} \\ &= \int_0^{2\pi} \cos[p(\theta - \mu)]dF(\theta) + i \int_0^{2\pi} \sin[p(\theta - \mu)]dF(\theta) \\ &= \cos(p\mu) + \int_0^{2\pi} p\{\sin[p(\theta - \mu)]\}F(\theta)d\theta - i \left\{ \sin(p\mu) + \int_0^{2\pi} p\{\cos[p(\theta - \mu)]\}F(\theta)d\theta \right\}.\end{aligned}$$

The first moment is given by

$$\mu_1 = \mathbb{E}[\cos(\Theta - \mu)] + i\mathbb{E}[\sin(\Theta - \mu)],$$

where

$$\mathbb{E}[\cos(\Theta - \mu)] = \cos(\mu) + \sum_{k=0}^{\infty} \sum_{s=0}^k T_{k,s} \left\{ A(\beta - k, 0, k - s + 1)M_0 + [\sin(\mu)]^{k-2s} A(\beta - k, 0, s + 1)M_1 \right\},$$

$$\mathbb{E}[\sin(\Theta - \mu)] = -\sin(\mu) - \sum_{k=0}^{\infty} \sum_{s=0}^k T_{k,s} \left\{ A(\beta - k, 1, k - s)M_0 - [\sin(\mu)]^{k-2s} A(\beta - k, 1, s)M_1 \right\}$$

and

$$A(a, b, c) = \int_0^{2\pi} \theta^a [\cos(\theta - \mu)]^b [\sin(\theta - \mu)]^c d\theta.$$

C Dataset

Table 8: 21 wind directions, at a weather station in Milwaukee, at 6.00am, on each of consecutive days [[Johnson and Wehrly \(1977\)](#)].

356	97	211	232	343	292	157	302	335	302	324
85	324	340	157	238	254	146	232	122	329	

References

- Abe, T. and Pewsey, A. (2013). Extending Circular Distributions through Transformation of Argument. *Annals of the Institute of Statistical Mathematics* **65**, 833–858.
- Abe, T. and Pewsey, A. (2009). Sine-skewed Circular Distributions. *Statistical Papers* **52**, 683–707.
- Abe, T., Pewsey, A. and Shimizu, K. (2009). On Papakonstantinou’s extension of the cardioid distribution. *Statistics and Probability Letters* **79**, 2138–2147.
- AL-Hussaini E. K. and Ahsanullah M. (2015). *Exponentiated Distributions*. Paris: Atlantis Press.
- Batschelet, E. (1981). *Circular Statistics in Biology*. New York: Academic Press.
- Boles, L.C. and Lohmann, K. J. (2003). True Navigation and Magnetic Maps in Spiny Lobsters. *Nature* **421**, 60–63.
- Box, G. E. P. and Pierce, D. A. (1970). Distribution of Residual Autocorrelations in Autoregressive-Integrated Moving Average Time Series Models. *Journal of the American statistical Association* **65**, 1509–1526.
- Fernández-Durán J. J (2007). Circular Distributions Based on Nonnegative Trigonometric Sums. *Biometrics* **60**, 499–503.
- Fisher, N. I. (1993). *Statistical analysis of circular data*. Cambridge: Cambridge University Press.
- Gatto R. and Jammalamadaka S. R. (2007). The Generalized von Mises Distribution. *Statistical Methodology* **4**, 341–353.

Jammalamadaka, S. R. and SenGupta, A. (2001). *Topics in Circular Statistics*. Singapore: World Scientific.

Jammalamadaka, S.R. and Sengupta, A. (1972). Mathematical Techniques for Paleocurrent Analysis: treatment of Directional Data. *Journal of the International Association for Mathematical Geology* **4**, 235–248.

Jeffreys, H. (1961). *Theory of Probability*, 3rd edn. Oxford: Clarendon Press.

Johnson, R. A. and Wehrly, T. E. (1977). Measures and models for angular correlation and angular-linear correlation. *Journal of the Royal Statistical Society* **39**, 222–229.

Jones, M. C. and Pewsey, A. (2012). Inverse Batschelet Distributions for Circular Data. *Biometrics* **68**, 183–193.

Kato, S. and Jones, M. C. (2010). A family of distributions on the circle with links to, and applications arising from, Möbius transformation. *Journal of the American Statistical Association* **105**, 249–262.

Mardia, K. V. (1972). *Statistics of Directional Data*. London-New York: Academic Press.

Pewsey, A., Neuhäuser, M. and Ruxton, G. D. (2013). *Circular statistics in R*, 3rd edn. Oxford: Oxford University Press.

R Core Team (2015). *R: A Language and Environment for Statistical Computing*. Vienna, Austria.